

Original article

Design, synthesis and biological evaluation of new potent 5-nitrofuryl derivatives as anti-*Trypanosoma cruzi* agents. Studies of trypanothione binding site of trypanothione reductase as target for rational design

Gabriela Aguirre ^a, Eliana Cabrera ^a, Hugo Cerecetto ^{a,*}, Rossanna Di Maio ^a, Mercedes González ^a, Gustavo Seoane ^a, Adelina Duffaut ^b, Ana Denicola ^c, María J. Gil ^d, Victor Martínez-Merino ^d

^a Departamento de Química Orgánica, Facultad de Química—Facultad de Ciencias, Iguá 4225, 11400 Montevideo, Uruguay

^b Liceo N° 1 Río Negro, Consejo de Enseñanza Secundaria, Fray Bentos, Uruguay

^c Laboratorio de Fisicoquímica Biológica, Facultad de Ciencias, Iguá 4225, 11400 Montevideo, Uruguay

^d Departamento de Química Aplicada, Universidad Pública de Navarra, 31006 Pamplona, Spain

Received 1 September 2003; received in revised form 21 February 2004; accepted 25 February 2004

Abstract

Design, using force-field calculations on the catalytic site of trypanothione reductase from *Trypanosoma cruzi*, has led to the development of new 5-nitrofuryl derivatives as potential anti-trypanosomal agents. The synthesized compounds were tested in vitro against *T. cruzi* and more than 75% of the prepared derivatives showed higher activity than nifurtimox. Compounds **5** and **11**, hexyl 4-(5-nitrofurfurylidene)carbazate and *N*-hexyl 3-(5-nitrofuryl)propanamide, showed the highest in vitro trypanocidal effect reported to date for members of the nitrofuran family. Partition coefficients and energies for the single-electron reduction of compounds were theoretically determined. These properties could be not the major cause of the activities' differences. The physicochemical environment around E19, W22, C53 and Y111 residues within the trypanothione binding site of trypanothione reductase resulted a valuable target for the rational design of anti-trypanosomal drugs.

© 2004 Elsevier SAS. All rights reserved.

Keywords: 5-Nitrofuryl derivatives; Anti-trypanosomal compounds; Structure–activity relationship

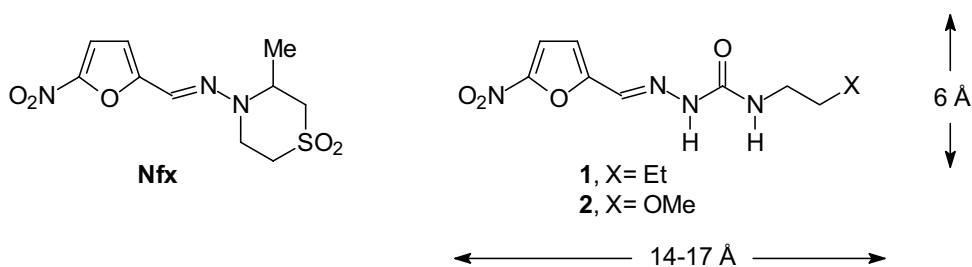
1. Introduction

A great deal of attention has been focused on developing efficient chemotherapeutic agents against Chagas' disease, which is produced by *Trypanosoma cruzi* [1–3]. Current treatment is based on benznidazole (a nitroimidazole derivative) or nifurtimox (a nitrofuran derivative, Nfx, Scheme 1), compounds that cause side effects and show poor clinical efficacy [4–7]. These two drugs are effective against the circulating form of the parasite (trypomastigotes) during the acute phase of the disease, but not during the chronic stage. There is, therefore, an urgent need for the development of effective agents acting at key targets in *T. cruzi*. One of them is trypanothione reductase (TR, EC 1.6.4.8) an NADPH-

dependent flavoenzyme responsible for many trypanosome protections against free radicals. TR occurs exclusively in trypanosomatids, which lack a glutathione reductase (hGR, EC: 1.6.4.2, the human equivalent anti oxidative stress enzyme), and many authors have indicated TR to be one of the most promising targets for research on trypanocidal drugs [8–11]. Thus, numerous papers have been published on the determination of the experimental inhibitory activity towards TR of several families of compounds and the relationships with their in vitro trypanocidal activity [10,12–16]. In general, these studies did not reveal any tangible correlation [10,12–14] or show major exceptions [16] between TR inhibition and in vitro trypanocidal effect against *T. cruzi*. Rapid transformations of the compounds in the biological medium [10,13,16] and drug delivery aspects, including cellular penetration [14,15] amongst others, have been postulated to explain the absence of the aforementioned straightforward correlation. It seems that the crucial parameter for a high

* Corresponding author.

E-mail addresses: hcerecet@fq.edu.uy (H. Cerecetto), merino@unavarra.es (V. Martínez-Merino).



Scheme 1. Nifurtimox and lead compounds.

trypanocidal activity is the combination of both redox cycling activity and inhibition of trypanothione reduction [12].

An alternative way to the experimental determination of key parameters in the design of potential anti-chagasic compounds could be the use of computational techniques to obtain theoretical properties related with those parameters. In this work, we present the design of anti-*T. cruzi* compounds by means of computational chemistry calculations and docking analysis on TR from *T. cruzi* (TcTR). Thus, the new 5-nitrofuryl derivatives designed were evaluated against epimastigote forms of *T. cruzi*, were also analyzed as potential ligands for TR and their lipophilicity and Gibbs free energies for the single-electron reduction were theoretically calculated.

We have selected nitrofuran derivatives for this study, because it is known [17] that they act as substrates for TR and they also effectively inhibit enzymatic reduction of trypanothione disulphide (the enzyme's physiological substrate). Members of this family of compounds, as nifuroxazide, nifuroxime or nifurpazine, are subversive substrates (turncoat inhibitors) of TR and they divert electrons from the physiologically catalyzed reactions, while the respective reaction with hGR is negligible [18]. Single-electron enzymatic reductions of nitro-aromatic compounds to their anion radicals are accompanied by futile redox cycling and oxidative stress, since nitro radicals are rapidly reoxidized by oxygen with the formation of superoxide. The trypanocidal activity of the most potent TR inhibitors seems to be related with the specific release of superoxide anion radicals in the parasite, a consequence of their redox cycling activity [12]. Indeed, this was the suggested mode of action of the nitrofuran derivatives as trypanocidals, exemplified by Nfx, which is reduced to the corresponding nitro anion radical by *T. cruzi* cells [19–22]. In agreement with the redox cycling behavior of nitrofuran derivatives, their electrochemical potentials were directly correlated with the oxygen uptake under mitochondrial respiratory inhibition by cyanide, but were not correlated with growth inhibition [23].

In this work, *N*⁴-butyl derivative of nitrofurazone (5-nitro-2-furaldehyde semicarbazone) **1** was selected as the lead compound (Scheme 1). We have recently explored nitrofurazone derivatives, where compounds **1** and **2** (Scheme 1) afforded the best anti-chagasic profile [24,25]. Moreover, nitrofurazone derivative **1** also proved to generate nitro anion radicals [26]. On the other hand, derivative **1** was a good example of the reported 3-D QSAR model on in vitro and in

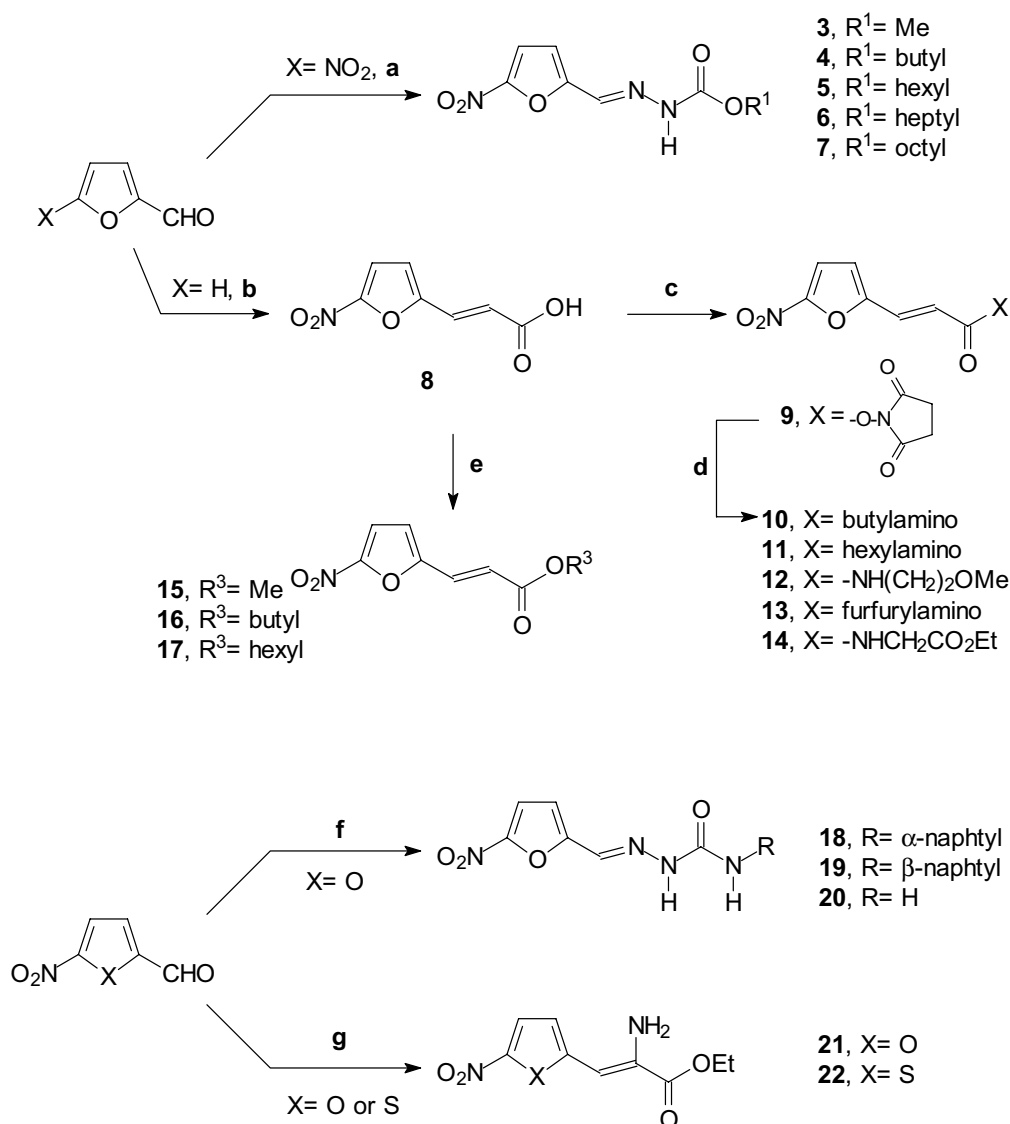
vivo anti-parasitic activities against *T. cruzi*, this in vitro model was found to be in agreement with the active site of TcTR [27].

2. Chemistry

2.1. Design

Initially, based in our 3-D QSAR model, we designed some 5-nitrofuryl derivatives with appropriate steric and electronic properties (Scheme 1) [27]. So, we proposed carbazates **4–5**, amides **10–11**, ester **16–17** and aminoesters **21–22** (Scheme 2). Further, we analyzed their capacity to interact with TR.

Reduction of 5-nitrofuryl derivatives may occur at the active site of TR, or at different sites as already suggested for chinifur [28]. Thus, we theoretically studied the docking concerning nitrofurazone derivative **1** on different TcTR sites. They showed that the active site (trypanothione site) was the most energetically favorable point of interaction between TcTR and nitrofurazone **1** (Fig. 1A) in detriment of the other known studied sites, i.e. the 'FAD site' [29], the 'NAD site' [30] and the 'third site' [31] (for details, see supplementary data). The most favorable disposition of **1** in terms of the active site of TcTR, as shown in Fig. 1A, is that in which the nitro group points towards the reactive hole (S15-water-C53-V54-T335-H461' residues). The semicarbazone group of **1** participates in two hydrogen bonds with E19 and Y111 residues, and its *N*-tail (butyl group) fills a hydrophobic hollow (W22-L18-M114). The distances (obtained from X-ray data) [29] between significant points of C53 (SH), Y111(OH), E19(COO⁻) and W22 (C₂H) residues of the site are 8.2 Å (SH...OH), 11.7 Å (SH...O⁻), 16.5 Å (SH...C₂H), 7.7 Å (OH...O⁻), and 10.0 Å (OH...C₂H) (Fig. 1B). The four points indicated above belong to the same plane (RMS distance of atoms from plane <0.01 Å). These four interaction points in TcTR seem suitable for use in the design of new trypanocidals because the active site of the human equivalent anti oxidative stress enzyme (hGR) is notably different. The disulphide holes in the TcTR and hGR catalytic sites have the same kind of residues, but sites differ in the fact that the anionic point in TcTR (E19 residue) is a cationic point in hGR (R347) and, furthermore, the lipophilic wall (W22) in TcTR is occupied by another cationic residue in hGR (R37) [29,32]. In agreement with these distances,



Scheme 2. Preparation of derivatives **3–22**: (a) H₂NHNCOR¹/toluene/*p*-TsOH/rt; (b) (1) malonic acid/Py/ Δ , (2) Ac₂O/HNO₃/H₂SO₄(c)/0 °C; (c) *N*-hydroxysuccinimide/DCC/CH₂Cl₂/0 °C to rt; (d) R²NH₂/CH₂Cl₂/rt; (e) R³OH(solvent)/*p*-TsOH/reflux; (f) H₂NHNCOR¹/toluene/*p*-TsOH/rt; (g) ethylglycinate hydrochloride/toluene/*p*-TsOH/rt.

carbazates **4–5** (Fig. 1C) or amides **10–11** (Fig. 1D) would give rise to good interactions with the active site of the enzyme on the same points as semicarbazone **1**. Docking study also showed that esters **16–17** despite losing a possible hydrogen bond with E19 could also connect with the enzyme, as shown by the data in Table 1 (*E*, binding energy, see Section 6). Even amino esters **21–22** (Table 1) could dock in the active site of TcTR in a similar way to **1**.

2.2. Synthesis

The designed compounds were synthesized along with some derivatives in which variations in the lipophilicity and/or in redox properties were done. Derivatives **3–22** were

prepared according to procedures depicts in Scheme 2. Carbazate derivatives **3–7** were obtained in a very clean process from the corresponding carbazate reactants (commercially available in the case of R¹ = Me or synthesized from the corresponding alcohol [33]). On the other hand, attempts to transform the acid **8** [34,35] into the amide derivatives **10–14** via the acyl chloride intermediate (using SOCl₂ [35]) led to complete decomposition of the starting material. One-pot procedures [36] using different activating agents generated the desired amides in very low yields or produced mixtures that proved difficult to separate (see Table 2 for derivative **11**). Furthermore, amides **10–14** were prepared by following a two-step procedure from the corresponding acid **8**, which was transformed into the intermediate **9** (Scheme 2). Treatment of intermediate **9** with different amines at room tem-

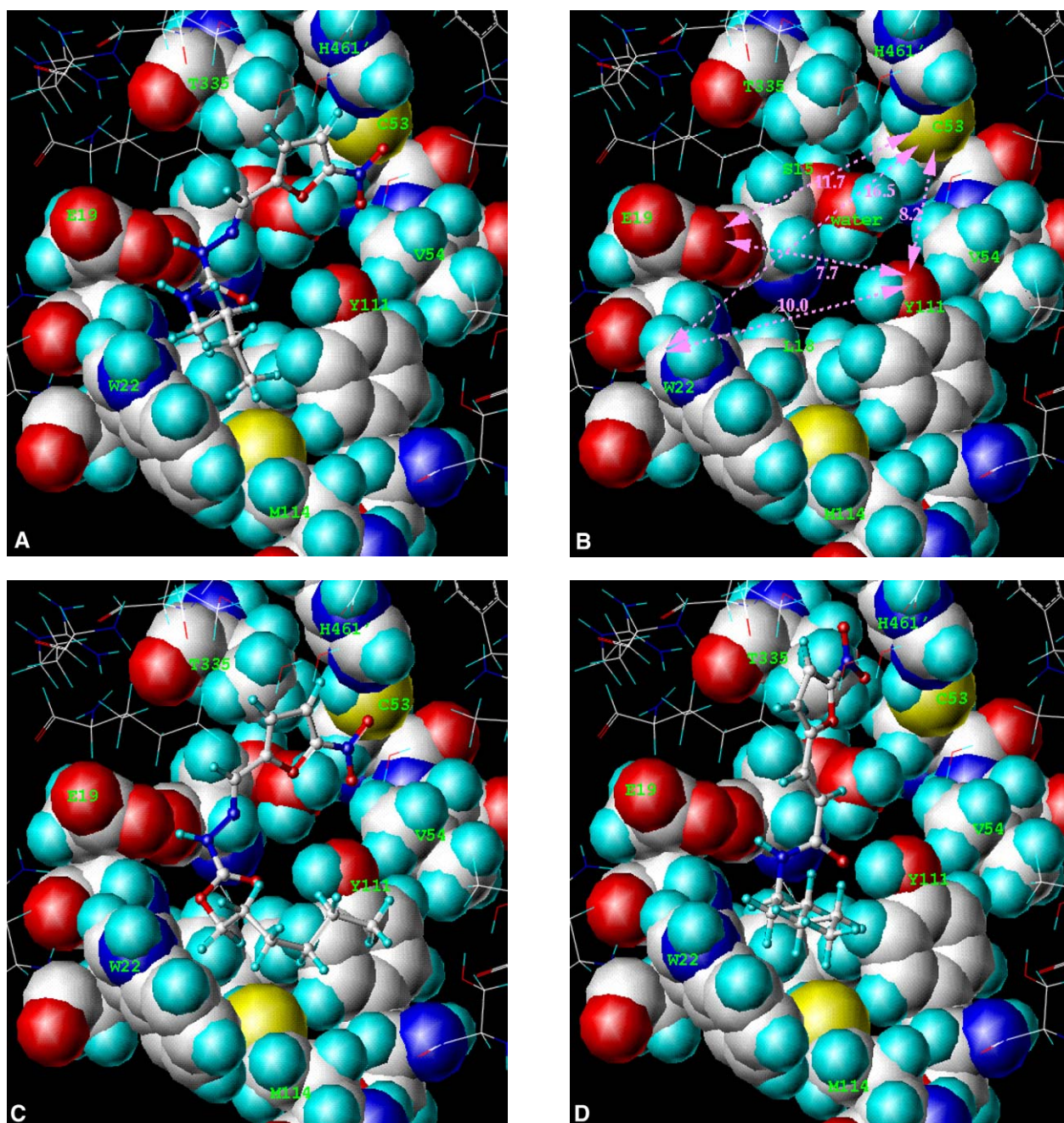


Fig. 1. (A) Dock of semicarbazone derivative 1, displayed in ball and stick format, into the trypanothione site of TR. Nearest residues are displayed in space filling format. (B) Main interaction residues within the trypanothione site of TcTR used in the design. Distances between significant points are in Å. (C) Dock of carbazate 5, displayed in ball and stick format, into the trypanothione site of TR. (D) Dock of amide 11, displayed in ball and stick format, into the trypanothione site of TR.

perature permit to obtain the desired products in moderate yields. The esters 15–17 were obtained in good yield by stirring 8 with the corresponding alcohol as solvent in an acid medium (Scheme 2). Semicarbazones 18–20 and aminoesters 21 and 22 were obtained by standard procedures (Scheme 2) [24,25,37]. The structures of all derivatives were confirmed by NMR (^1H , ^{13}C , and HETCOR experiments), IR and MS, and their purities were established by TLC and microanalysis.

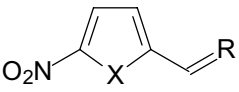
3. Pharmacology

3.1. Anti-trypanosomal studies

The compounds were tested in vitro against epimastigote forms of *T. cruzi* (Tulahuen strain) at 5, 10 and 25 μM , as indicated in Section 6 [38,39]. Table 3 shows the percentage of inhibition for the evaluated derivatives at 5 μM . We used the no infective epimastigote form, as has been done in several other studies with other nitrofurans and nitroimidazole

Table 1

Docking energies in the trypanothione site of TcTR (E), maximum length (L) and Gibbs free energy of single electron reduction [$\Delta G(L^-)$] for designed compounds



X	R	E (kcal mol ⁻¹) ^a	L (Å) ^b	$\Delta G(L^-)$ (kcal mol ⁻¹) ^c
Compounds				
1	O =N–NH–CO–NH(CH ₂) ₃ CH ₃	-34.06	15.6	-46.81
2	O =N–NH–CO–NH(CH ₂) ₂ OCH ₃	-31.93	18.2	-47.18
4	O =N–NH–CO–O(CH ₂) ₃ CH ₃	-29.11	16.0	-47.95
5	O =N–NH–CO–O(CH ₂) ₅ CH ₃	-30.74	18.6	-49.15
10	O =CH–CO–NH(CH ₂) ₃ CH ₃	-32.55	15.2	-51.62
11	O =CH–CO–NH(CH ₂) ₅ CH ₃	-34.60	17.7	-51.64
16	O =CH–CO–O(CH ₂) ₃ CH ₃	-25.68	15.0	-54.53
17	O =CH–CO–O(CH ₂) ₅ CH ₃	-23.34	17.5	-54.80
21	O =C(NH ₂)–CO–OCH ₂ CH ₃	-23.26	11.9	-48.74
22	S =C(NH ₂)–CO–OCH ₂ CH ₃	-25.65	12.5	-54.09

^a Energy of the ligand–cavity binding from Tripos force field within the SYBYL-DOCK program.

^b Maximum length of the ligand in its extended conformation.

^c Gibbs free energy of single-electron reduction of ligand from AM1 method at 298 K in the gas phase.

derivatives as well as other natural and synthetic potential trypanocidal agents, which have also proved to be efficient against the trypomastigote and amastigote forms [40]. The existence of the epimastigote form as an obligate mammalian intracellular stage has been revisited [41,42] and confirmed recently [43]. ED₅₀, 50% effective doses to inhibit the parasite growth, values were determined for derivatives **1**, **5**, and **11** (Table 4 and Fig. 2).

3.2. Theoretical determinations

The partition coefficients (log P) for all derivatives were calculated using $C \log P$ 4.0 (Table 3) [44]. The Gibbs free energies of the single-electron reductions of the designed

Table 3

Anti-trypanosomal in vitro activity (% Inh.), binding energy in the active site of TcTR including desolvation terms (BE) and octanol/water partition coefficient (log P) of developed compounds



X	R	% Inh. ^{a,b} (5 μM)	BE ^c (kcal mol ⁻¹)	LogP ^d [44]
Compounds				
1	O =N–NH–CO–NH(CH ₂) ₃ CH ₃	30.0	-41.89	1.94
2	O =N–NH–CO–NH(CH ₂) ₂ OCH ₃	20.0	-35.32	0.26
3	O =N–NH–CO–OCH ₃	32.0	-27.28	-0.37
4	O =N–NH–CO–O(CH ₂) ₃ CH ₃	84.2	-40.02	1.22
5	O =N–NH–CO–O(CH ₂) ₅ CH ₃	96.2	-47.79	2.27
6	O =N–NH–CO–O(CH ₂) ₆ CH ₃	92.7	-52.94	2.80
7	O =N–NH–CO–O(CH ₂) ₇ CH ₃	83.7	-57.06	3.33
8	O =CH–CO–OH	20.0	-13.27	1.16 (0.68)
9	O =CH–CO–O–(1-succinimidyl)	6.0	-25.12	0.00
10	O =CH–CO–NH(CH ₂) ₃ CH ₃	75.0	-34.00	2.31 (2.36)
11	O =CH–CO–NH(CH ₂) ₅ CH ₃	82.0	-47.14	3.37
12	O =CH–CO–NH(CH ₂) ₂ OCH ₃	31.0	-29.45	0.74
13	O =CH–CO–NHCH ₂ (2-furyl)	14.0	-30.29	1.67
14	O =CH–CO–NHCH ₂ –CO–OCH ₂ CH ₃	35.0	-27.73	1.19
15	O =CH–CO–OCH ₃	39.0	-22.22	1.53 (1.65)
16	O =CH–CO–O(CH ₂) ₃ CH ₃	42.0	-33.90	3.12 (2.83)
17	O =CH–CO–O(CH ₂) ₅ CH ₃	17.0	-42.69	4.18
18	O =N–NH–CO–NH(α -naphthyl)	32.0	-48.99	3.43
19	O =N–NH–CO–NH(β -naphthyl)	59.0	-49.01	3.43
20	O =N–NH–CO–NH ₂	67.0	-21.82	0.20 (0.23)
21	O =C(NH ₂)–CO–OCH ₂ CH ₃	n.a. ^e	-20.99	1.30
22	S =C(NH ₂)–CO–OCH ₂ CH ₃	9.0	-30.37	1.86

^a Values are means of two experiments.

^b % Inh. = percentage of inhibition of *T. cruzi* growth at a dosage of 5 μM at day 5.

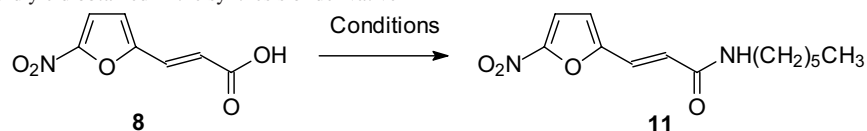
^c Binding energy from the SYBYL-LEAPFROG program including the desolvation of ligand and cavity.

^d Calculated log P (measured value in parenthesis) from Clog P 4.0.

^e n.a. = not active at 5 μM.

Table 2

One pot conditions assayed and yield obtained in the synthesis of derivative **11**



Conditions	Yield (%)
(1) DCC /CH ₂ Cl ₂ /rt; (2) hexylamine/CH ₂ Cl ₂ /rt	14 ^b
(1) DCC/1-hydroxybenzotriazole/CH ₂ Cl ₂ /rt; (2) hexylamine/CH ₂ Cl ₂ /rt	20 ^b
(1) CDI /CH ₂ Cl ₂ /rt; (2) hexylamine/CH ₂ Cl ₂ /rt	10
(1) ClCO ₂ Et/Et ₃ N/THF/-8 °C; (2) hexylamine/THF/0 °C to rt	4

^a DCC: dicyclohexylcarbodiimide.

^b Compound **11** is contaminated with dicyclohexylurea.

^c CDI: carbonyldiimidazole.

Table 4
ED₅₀ values and calculated parameters for the most active alkyl derivatives of each tested family of 5-nitrofuryl derivatives

Compounds	Family	ED ₅₀ (μM)	BE (kcal mol ⁻¹) ^a	ΔG(L ⁻)(kcal mol ⁻¹) ^b	LogP ^c
1	Semicarbazone	7.4 ± 0.5 ^d	-41.89	-46.8	1.94
5	Carbazate	3.2 ± 0.5 ^d	-47.79	-49.2	2.27
11	Amide	2.0 ± 0.5 ^d	-47.14	-51.6	3.37
16	Ester	> 5 ^e	-33.90	-54.5	3.12
21	Amino-ester	> 10 ^e	-20.99	-48.7	1.30

^a TcTR cavity–ligand binding energies from the LEAPFROG module of SYBYL.

^b Gibbs free energy of single-electron reduction of ligand from AM1 method at 298 K in the gas phase.

^c Calculated from C log P version 4.0.

^d Values are means of two experiments.

^e Values estimated.

ligands [ΔG(L⁻)] were estimated using the AM1 method in the gas phase at 298 K. This kind of calculation offers a good correlation with corresponding experimental single-electron reduction potentials of nitroaromatics [45]. Esters **16** and **17**, amides **10** and **11**, carbazates **4** and **5** and amino-ester **21**, in decreasing order, present more favorable single-electron reductions than the corresponding 5-nitrofurfurylidene-semicarbazides **1** and **2**, as shown by the data in Table 1.

Additional ligand–cavity binding energies, including ligand and cavity desolvation terms (BE in Table 3), were estimated by means of the LEAPFROG module of SYBYL [46] from DOCK solutions. More negative BEs implicate more favorable compounds' binding energy in the trypanothione site of TcTR. In a previous test, LEAPFROG gave a good reproduction of the SM2-AM1 [47] desolvation energies of small molecules (Section 6). Moreover, ligand–cavity binding energies from LEAPFROG are a good approximation to reproduce K_i ligand–enzyme binding, as it has been demonstrated for some NADPH-dependent enzymes [48,49].

4. Results and discussion

New 5-nitrofuryl derivatives were developed as potential anti-trypanosomal agents. The majority of these compounds showed complete inhibition of the parasite growth at a dosage of 10 and 25 μM (data not shown). Some of the newly developed 5-nitrofuryl derivatives displayed better anti-

trypanosomal activity than Nfx at 5 μM (Nfx inhibition: 30.0%), i.e. compounds **4–7**, **10**, **11**, **16**, **19** and **20** (Table 3). ED₅₀ values were determined for the most active carbazate and amide derivatives. Carbazate **5** and amide **11** proved to be one of the most active novel compounds against epimastigote form of *T. cruzi* strain Tulahuén, with ED₅₀ values (3.2 and 2.0 μM, respectively) better than that observed for Nfx (7.7 μM). These compounds could be more effective in the infective and intracellular replicative forms since the molecular weight thiol content in the trypomastigote and amastigote forms of *T. cruzi* is lower than in epimastigote form [23,50].

The new 5-nitrofuryl derivatives reported here comply with some of the reported conditions to be good trypanocidals, they are potentially substrates for TcTR and show even more favorable single-electron reduction than derivative **1** (cathodic peak potential $E_{pc} = -0.86$ V [25], ΔG(L⁻) = -46.81 kcal mol⁻¹) and Nfx ($E_{pc} = -0.91$ V [24], ΔG(L⁻) = -46.08 kcal mol⁻¹), as can be deduced from the corresponding ΔG(L⁻) (Table 1). However, only the Gibbs free energy of the single-electron reduction (ΔG(L⁻) in Table 1) of the 5-nitrofuryl derivatives does not explain their differences as trypanocidals, at 5 μM. This could be in agreement with a redox cycling behavior of the compounds, as has been recently reported for the nitrofurazone **20** [23]. The experimental trypanocidal data shown in Table 3 confirm that the most active trypanosome growth inhibitors, at 5 μM, have the highest binding energies (BE) in the trypanothione site of TcTR (see also Fig. 3). It is important to note that energies from LEAPFROG (including the cavity and ligand desolvation, BE in Table 3) showed some relation with the inhibitory activity, at 5 μM, than energies from DOCK, where desolvation was not taken into account (E in Table 1). It should be noted that the metabolism of the compounds cannot be discarded as an explanation of some inhibition differences between families with similar BE values (Fig. 3).

On the other hand, the passive transport for all compounds does not seem to be related to biological response (see log P and % Inh. in Table 3). However, within each assayed family of derivatives appears a clear relation between log P and activity at 5 μM. In the family of alkyl carbazates **3–7**, it can be observed that there is an optimum partition coefficient value (at about 2.3) to obtain the highest inhibition. The most

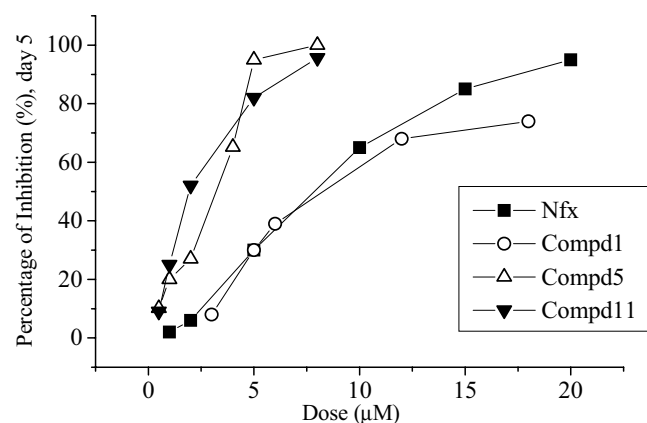


Fig. 2. Curves dose–response of Nfx and derivatives **1**, **5**, and **11**.

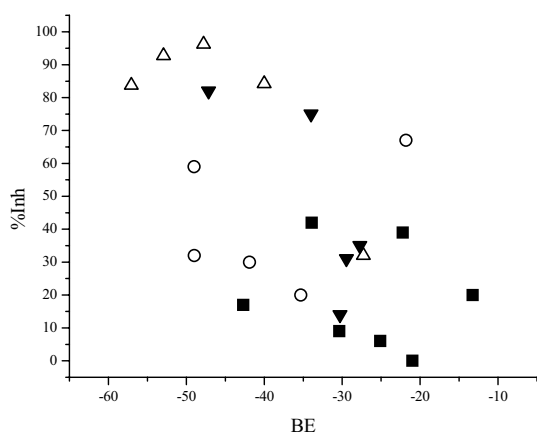


Fig. 3. Percentage of trypanosome growth inhibition at a dosage of 5 μM (% Inh.) vs. TcTR cavity–ligand binding energies from LEAPFROG calculations (BE). Semicarbazones are displayed as \circ , amides as ∇ , carbazates as \triangle and the rest of compounds as \blacksquare .

active examples of the assayed amides and esters also have their log P near to the aforementioned value (see activity of compound **11** and activity of compound **16**).

5. Conclusions

Thirteen of the 17 new derivatives developed in this work showed better trypanocidal effect against epimastigote forms of *T. cruzi* than nifurtimox at 5 μM . These compounds showed the highest in vitro trypanocidal effect reported to date for members of the nitrofuran family of compounds. The method employed by us, which detects different micro-orientations for the ligands on the TcTR site, renders a design of trypanocidals that is as good as others based on the experimental inhibition of TR. Compounds that bind in the trypanothione site of TcTR and also bring favorable energy of the single-electron reduction and adequate log P showed good trypanocidal activity.

Studies related with activity and toxicity in vivo with the more active derivatives are currently in progress.

6. Experimental protocols

6.1. Chemistry

All starting materials were commercially available research-grade chemicals and used without further purification. The compounds **8**, **20–22**, 4-(1-naphthyl) semicarbazide, 4-(2-naphthyl)-semicarbazide, butyl-, hexyl-, heptyl-, and octylcarbazate were prepared according to literature procedures [33–35,37,51]. All solvents were dried and distilled prior to use. All the reactions were carried out in a nitrogen atmosphere. The typical work-up included washing with brine and drying the organic layer with sodium sulphate before concentration. Melting points were determined using a Leitz Microscope Heating Stage Model 350 apparatus and are uncorrected. Elemental analyses were

obtained from vacuum-dried samples (over phosphorous pentoxide at 3–4 mm Hg, 24 h at room temperature) and performed on a Fisons EA 1108 CHNS-O analyzer. Infrared spectra were recorded on a Perkin–Elmer 1310 apparatus, using potassium bromide tablets; the frequencies are expressed in cm^{-1} . $^1\text{H-NMR}$ and $^{13}\text{C-NMR}$ spectra were recorded on a Bruker DPX-400 (at 400 and 100 MHz) instrument, with tetramethylsilane as the internal reference and in the indicated solvent; the chemical shifts are reported in ppm. J values are given in Hertz. Mass spectra were recorded on a Shimadzu GC-MS QP 1100 EX instrument at 70 eV.

6.1.1. General procedure for the synthesis of carbazates 3–7

A mixture of 5-nitro-2-furaldehyde (1 eq.), the corresponding carbazate (1 eq.), *p*-TsOH (catalytic amounts) and toluene as solvent was stirred at room temperature until the carbonyl compound was not present (SiO_2 , 1% MeOH in CH_2Cl_2). The resulting precipitate was collected by filtration and was crystallized with the indicated solvent.

6.1.1.1. Methyl 4-(5-nitrofurfurylidene)carbazate (3). Yellow-orange solid (60%); mp 205.0–207.0 $^\circ\text{C}$ (from petroleum ether: EtOAc) (Found: C, 39.4; H, 3.3; N, 19.7. $\text{C}_7\text{H}_7\text{N}_3\text{O}_5$ requires C, 39.4; H, 3.3; N, 19.7); δ_{H} (400 MHz, DMSO- d_6) 3.73 (3H, s, O- CH_3), 7.14 (1H, d, J 3.9, furan- H), 7.74 (1H, d, J 3.9, furan- H), 7.97 (1H, s, $-\text{CH}=\text{N}$) and 11.54 (1H, br s, NH); δ_{C} (100 MHz, DMSO- d_6) (HMQC, HMBC) 54.50 ($-\text{CH}_3$), 115.50 (furan-C), 116.50 (furan-C), 134.20 ($\text{H}-\text{C}=\text{N}$), 152.17 (furan-C), 153.48 (furan-C) and 154.78 ($-\text{C}=\text{O}$). m/z 213 (M^+ , 100.0%), 197 (2.5), 182 (1.8) and 167 (12.6).

6.1.1.2. Butyl 4-(5-nitrofurfurylidene)carbazate (4). Yellow-orange needles (38%); mp 147.6–148.5 $^\circ\text{C}$ (from EtOH:H $_2$ O) (Found: C, 47.05; H, 5.1; N, 16.3. $\text{C}_{10}\text{H}_{13}\text{N}_3\text{O}_5$ requires C, 47.1; H, 5.1; N, 16.46); δ_{H} (400 MHz, CDCl_3) 0.96 (3H, t, J 7.4, $-\text{CH}_3$), 1.42 (2H, sextet, J 7.4, $-\text{CH}_2$), 1.69 (2H, quintet, J 6.8, $-\text{CH}_2$), 4.26 (2H, t, J 6.7, O- CH_2), 7.00 (1H, d, J 3.8, furan- H), 7.36 (1H, d, J 3.8, furan- H), 8.05 (1H, br s, $-\text{CH}=\text{N}$) and 8.62 (1H, br s, NH); δ_{C} (100 MHz, CDCl_3) (HMQC, HMBC) 14.04 ($-\text{CH}_3$), 19.35 ($-\text{CH}_2$), 31.20 ($-\text{CH}_2$), 66.83 ($-\text{CH}_2$), 112.30 (furan-C), 113.69 (furan-C), 132.00 ($\text{H}-\text{C}=\text{N}$), 152.25 (furan-C), 152.50 (furan-C) and 153.00 ($-\text{C}=\text{O}$); m/z 255 (M^+ , 22.9%), 239 (0.5) and 182 (24.9).

6.1.1.3. Hexyl 4-(5-nitrofurfurylidene) carbazate (5). Yellow-orange needles (50%); mp 139.9–140.8 $^\circ\text{C}$ (from EtOH:H $_2$ O) (Found: C, 50.85; H, 6.2; N, 14.8. $\text{C}_{12}\text{H}_{17}\text{N}_3\text{O}_5$ requires C, 50.9; H, 6.05; N, 14.8); δ_{H} (400 MHz, CDCl_3) 0.92 (3H, t, J 6.8, $-\text{CH}_3$), 1.39 (6H, m, $-\text{CH}_2$), 1.71 (2H, quintet, J 7.0, $-\text{CH}_2$), 4.27 (2H, t, J 6.7, O- CH_2), 7.01 (1H, d, J 3.8, furan- H), 7.38 (1H, d, J 3.8, furan- H), 8.08 (1H, br s, $-\text{CH}=\text{N}$) and 8.46 (1H, br s, NH); δ_{C} (100 MHz, CDCl_3) (HMQC, HMBC) 14.34 ($-\text{CH}_3$), 22.90 ($-\text{CH}_2$), 25.78 ($-\text{CH}_2$), 29.14 ($-\text{CH}_2$), 31.77 ($-\text{CH}_2$), 67.11 ($-\text{CH}_2$), 112.28

(furan-C), 113.65 (furan-C), 132.77 (H–C=N), 152.22 (furan-C), 153.00 (furan-C) and 153.50 (–C=O); m/z 283 (M^+ , 53.7%), 267 (0.8) and 182 (14.3).

6.1.1.4. Heptyl 4-(5-nitrofurfurylidene)carbazate (6). Yellow needles (45%); mp 121.9–123.0 °C (from petroleum ether: EtOAc) (Found: C, 52.6; H, 6.3; N, 14.3. $C_{13}H_{19}N_3O_5$ requires C, 52.5; H, 6.4; N, 14.1); ν_{max} 3221.5, 1743.9, 1230.7 and 819.8; δ_H (400 MHz, $CDCl_3$) 0.89 (3H, t, J 7.1, – CH_3), 1.30 (8H, m, – CH_2), 1.69 (2H, quintet, J 6.9, – CH_2), 4.24 (2H, t, J 6.7, O– CH_2), 7.00 (1H, d, J 3.8, furan- H), 7.36 (1H, d, J 3.8, furan- H), 8.05 (1H, br s, – $CH=N$) and 8.50 (bs, 1H, NH); m/z 297 (M^+ , 8.8%), 267 (0.1) and 182 (3.6).

6.1.1.5. Octyl 4-(5-nitrofurfurylidene)carbazate (7). Yellow needles (61%); mp 118.3–119.6 °C (from petroleum ether: EtOAc) (Found: C, 53.9; H, 6.7; N, 13.3. $C_{14}H_{21}N_3O_5$ requires C, 54.0; H, 6.75; N, 13.5); ν_{max} 3219.6, 1747.7, 1226.8 and 810.0; δ_H (400 MHz, acetone- d_6) 0.88 (3H, t, J 7.1, – CH_3), 1.31 (10H, m, – CH_2), 1.67 (2H, quintet, J 6.6, – CH_2), 4.18 (2H, t, J 6.6, O– CH_2), 7.07 (1H, d, J 3.9, furan- H), 7.58 (1H, d, J 3.9, furan- H), 8.16 (1H, br s, – $CH=N$) and 10.43 (1H, br s, NH); m/z 311 (M^+ , 10.7%), 282 (0.2) and 182 (4.8).

6.1.2. N-[3-(5-Nitrofuryl)-2-propenyl]oxysuccinimide (9)

A mixture of acid **8** (0.50 g, 2.7 mmol) and *N*-hydroxysuccinimide (0.31 g, 2.7 mmol) in dry CH_2Cl_2 (10.0 cm^3) was stirred at 0 °C (ice/water), then DCC (0.56 g, 2.7 mmol) was added. The reaction mixture was allowed to stir for a further 1 h at 0 °C and 24 h at room temperature. The solid (dicyclohexylurea) was collected by filtration, washed with CH_2Cl_2 and the filtrate concentrated under reduced pressure. The resulting solid was washed with hot ethanol:petroleum ether (1:1). Beige solid (0.34 g, 45%); mp 210.0 °C (d) (Found: C, 47.0; H, 2.5; N, 10.3. $C_{11}H_8N_2O_7$ requires C, 47.1; H, 2.9; N, 10.0); δ_H (400 MHz, $CDCl_3$) 2.88 (4H, s, – CH_2), 6.80 (1H, d, J 15.9, = $CH-$), 6.89 (1H, d, J 3.8, furan- H), 7.36 (1H, d, J 3.8, furan- H) and 7.62 (1H, d, J 15.9, = $CH-$); m/z 280 (M^+ , 1.4%), 264 (0.1) and 166 (100.0).

6.1.3. General procedure for the synthesis of amides 10–14

A mixture of intermediate **9** (1 eq.), the corresponding amine (1.2 eq.) and dry CH_2Cl_2 as solvent was stirred at room temperature until the compound **9** was not present (SiO_2 , 40% EtOAc in petroleum ether). The mixture was concentrated in vacuo and treated with EtOAc. After the work-up process the residue was purified as indicate.

6.1.3.1. N-Butyl 3-(5-nitrofuryl)propenamide (10). Chromatographic column (SiO_2 , petroleum ether:EtOAc (0–20%)); yellow oil (51%); (Found: C, 55.2; H, 5.6; N, 11.55. $C_{11}H_{14}N_2O_4$ requires C, 55.5; H, 5.9; N, 11.8); ν_{max} 3271.7, 1662.8 and 814.1; δ_H (400 MHz, $CDCl_3$) 0.96 (3H, t, J 7.3, – CH_3), 1.41 (2H, sextet, J 7.4, – CH_2), 1.58 (2H, quintet, J 7.1, – CH_2), 3.42 (2H, q, J 7.0, N– CH_2), 5.96 (1H,

br s, NH), 6.67 (1H, d, J 15.3, = $CH-$), 6.69 (1H, d, J 3.7, furan- H), 7.34 (1H, d, J 3.7, furan- H) and 7.41 (1H, d, J 15.3, = $CH-$); δ_C (100 MHz, $CDCl_3$) (HMQC, HMBC) 14.07 (– CH_3), 20.45 (– CH_2), 31.94 (– CH_2), 40.14 (– CH_2), 113.59 (furan-C), 115.11 (furan-C), 125.74 (– $CH=$), 125.93 (– $CH=$), 152.44 (furan-C), 153.58 (furan-C) and 164.53 (– $C=O$); m/z 238 (M^+ , 8.2%), 221 (4.8) and 166 (100.0).

6.1.3.2. N-Hexyl 3-(5-nitrofuryl)propenamide (11). Chromatographic column (SiO_2 , petroleum ether:EtOAc (0–20%)); brown-orange solid (48%); mp 102.5–104.0 °C (Found: C, 53.75; H, 6.8; N, 10.4. $C_{13}H_{18}N_2O_4$ requires C, 53.8; H, 6.8; N, 10.5); ν_{max} 3275.5, 1655.1 and 817.9; δ_H (400 MHz, $CDCl_3$) 0.92 (3H, t, J 6.7, – CH_3), 1.34 (4H, m, – CH_2), 1.58 (4H, m, – CH_2), 3.41 (2H, q, J 7.1, N– CH_2), 5.79 (1H, br s, NH), 6.66 (1H, d, J 15.3, = $CH-$), 6.70 (1H, d, J 3.8, furan- H), 7.34 (1H, d, J 3.7, furan- H) and 7.42 (1H, d, J 15.3, = $CH-$). m/z 266 (M^+ , 4.7%), 249 (7.8) and 166 (100.0).

6.1.3.3. N-(2-Methoxyethyl) 3-(5-nitrofuryl)propenamide (12). Chromatographic column (SiO_2 , petroleum ether:EtOAc (0–10%)); yellow-orange solid (40%); mp 125.0–126.7 °C (Found: C, 49.9; H, 5.1; N, 11.6. $C_{10}H_{12}N_2O_5$ requires C, 50.0; H, 5.0; N, 11.7); δ_H (400 MHz, $CDCl_3$) 3.42 (3H, s, O– CH_3), 3.54 (2H, t, J 5.2, – CH_2), 3.61 (2H, q, J 5.9, N– CH_2), 6.16 (1H, br s, NH), 6.68 (1H, d, J 15.1, = $CH-$), 6.70 (1H, d, J 3.4, furan- H), 7.34 (1H, d, J 3.8, furan- H) and 7.43 (1H, d, J 15.3, = $CH-$); δ_C (100 MHz, $CDCl_3$) (HMQC, HMBC) 40.00 (– CH_3), 59.19 (– CH_2), 71.25 (– CH_2), 113.50 (furan-C), 115.13 (furan-C), 125.54 (– $CH=$), 126.15 (– $CH=$), 152.40 (furan-C), 153.49 (furan-C) and 164.53 (– $C=O$); m/z 240 (M^+ , 7.2%), 208 (10.0) and 166 (100.0).

6.1.3.4. N-Furfuryl 3-(5-nitrofuryl)propenamide (13). Chromatographic column (SiO_2 , petroleum ether:EtOAc (0–40%)); oil (43 %) (Found: C, 54.75; H, 3.5; N, 10.3. $C_{12}H_{10}N_2O_5$ requires C, 55.0; H, 3.8; N, 10.7); δ_H (400 MHz, $CDCl_3$) 4.59 (2H, d, J 5.6, N– CH_2), 6.29 (1H, d, J 3.1, furan- H), 6.34 (2H, m, NH + furan- H), 6.69 (1H, d, J 15.8, = $CH-$), 6.71 (1H, d, J 3.1, furan- H), 7.33 (1H, d, J 3.8, furan- H), 7.38 (1H, dd, J_1 3.1, J_2 1.0, furan- H) and 7.43 (1H, d, J 15.3, = $CH-$); δ_C (100 MHz, $CDCl_3$) (HMQC, HMBC) 37.30 (– CH_2), 108.22 (furan-C), 110.94 (furan-C), 113.53 (furan-C), 115.40 (furan-C), 125.06 (– $CH=$), 126.60 (– $CH=$), 142.81 (furan-C), 151.01 (furan-C), 152.50 (furan-C), 153.34 (furan-C) and 164.42 (– $C=O$); m/z 262 (M^+ , 0.9%), 245 (2.1) and 166 (8.2).

6.1.3.5. N-(Ethylloxycarbonylmethyl) 3-(5-nitrofuryl)propenamide (14). Chromatographic column (SiO_2 , petroleum ether:EtOAc (0–40%)); beige solid (21%); mp 195.5–196.7 °C (Found: C, 49.05; H, 4.15; N, 10.5. $C_{11}H_{12}N_2O_6$ requires C, 49.25; H, 4.5; N, 10.45); ν_{max} 3358.5, 1720.7, 1672.5 and 831.4; δ_H (400 MHz, $CDCl_3$) 1.33 (3H, t, J 7.1, – CH_3), 4.19 (2H, d, J 5.1, N– CH_2), 4.25 (2H, q, J 7.1, O– CH_2), 6.35 (1H, br s, NH), 6.72 (1H, d, J 3.6, furan- H), 6.74 (1H, d, J 15.4, = $CH-$), 7.34 (1H, d, J 3.7, furan- H) and

7.44 (1H, d, J 15.4, =CH–); δ_C (100 MHz, CDCl₃) (HMQC, HMBC) 14.52 (–CH₃), 42.17 (–CH₂), 62.19 (–CH₂), 113.42 (furan-C), 115.47 (furan-C), 124.55 (–CH=), 126.85 (–CH=), 151.50 (furan-C), 153.19 (furan-C), 164.49 (–C=O) and 169.92 (–C=O); m/z 268 (M⁺, 2.6%), 222 (71.2) and 166 (100.0).

6.1.4. General procedure for the synthesis of esters 15–17

A mixture of intermediate **8**, *p*-toluenesulphonic acid (catalytic amounts) and the corresponding alcohol as solvent was heated at reflux until the compound **8** was not present (SiO₂, 40% EtOAc in petroleum ether). The mixture was concentrated in vacuo and treated with EtOAc. After the work-up process the residue was purified as indicated.

6.1.4.1. Ethyl 3-(5-nitrofuryl)propenoate (15). Chromatographic column (SiO₂, petroleum ether:EtOAc (0–10%)); beige solid (67%); mp 128.8–130.4 °C (Found: C, 51.1; H, 4.2; N, 6.6. C₉H₉NO₅ requires C, 51.2; H, 4.3; N, 6.6); δ_H (400 MHz, CDCl₃) 1.36 (3H, t, J 7.1, –CH₃), 4.30 (2H, t, J 7.1, O–CH₂), 6.66 (1H, d, J 15.9, =CH–), 6.77 (1H, d, J 3.7, furan-*H*), 7.34 (1H, d, J 3.8, furan-*H*) and 7.43 (1H, d, J 15.9, =CH–); m/z 211 (M⁺, 50.9%), 195 (1.6) and 166 (89.7).

6.1.4.2. Butyl 3-(5-nitrofuryl)propenoate (16). Chromatographic column (SiO₂, petroleum ether:EtOAc (0–30%)); oil (32%) (Found: C, 55.0; H, 5.2; N, 5.4. C₁₁H₁₃NO₅ requires C, 55.2; H, 5.4; N, 5.9); δ_H (400 MHz, CDCl₃) 0.98 (3H, t, J 7.4, –CH₃), 1.44 (2H, sextet, J 7.3, –CH₂), 1.71 (2H, quintet, J 7.1, –CH₂), 4.24 (2H, t, J 6.6, O–CH₂), 6.66 (1H, d, J 15.9, =CH–), 6.77 (1H, d, J 3.8, furan-*H*), 7.35 (1H, d, J 3.8, furan-*H*) and 7.42 (1H, d, J 15.9, =CH–); δ_C (100 MHz, CDCl₃) (HMQC, HMBC) 14.05 (–CH₃), 19.52 (–CH₂), 31.03 (–CH₂), 65.45 (–CH₂), 113.23 (furan-C), 115.52 (furan-C), 123.31 (–CH=), 129.02 (–CH=), 151.00 (furan-C), 152.86 (furan-C) and 166.07 (–C=O); m/z 239 (M⁺, 25.0%), 223 (0.8) and 166 (100.0).

6.1.4.3. Hexyl 3-(5-nitrofuryl)propenoate (17). Chromatographic column (SiO₂, petroleum ether); oil (45%) (Found: C, 58.3; H, 6.2; N, 5.0. C₁₃H₁₇NO₅ requires C, 58.4; H, 6.4; N, 5.2); δ_H (400 MHz, CDCl₃) 0.92 (3H, t, J 6.7, –CH₃), 1.31–1.43 (6H, m, –CH₂), 1.69 (2H, quintet, J 6.9, –CH₂), 4.23 (2H, t, J 6.7, O–CH₂), 6.66 (1H, d, J 15.9, =CH–), 6.77 (1H, d, J 3.7, furan-*H*), 7.35 (1H, d, J 3.7, furan-*H*) and 7.42 (1H, d, J 15.9, =CH–); δ_C (100 MHz, CDCl₃) (HMQC, HMBC) 14.34 (–CH₃), 22.90 (–CH₂), 25.96 (–CH₂), 28.96 (–CH₂), 31.79 (–CH₂), 65.75 (–CH₂), 113.25 (furan-C), 115.54 (furan-C), 123.30 (–CH=), 129.02 (–CH=), 152.00 (furan-C), 152.87 (furan-C) and 166.07 (–C=O); m/z 267 (M⁺, 13.1%), 251 (2.0) and 166 (100.0).

6.1.5. General procedure for the synthesis of semicarbazones 18 and 19

A mixture of 5-nitro-2-furaldehyde (1 eq.), the corresponding semicarbazide (1 eq.), *p*-TsOH (catalytic amounts) and toluene as solvent was stirred at room temperature until

the carbonyl compound was not present (SiO₂, 1% MeOH in CH₂Cl₂). The resulting precipitate was collected by filtration and was crystallized with the indicated solvent.

6.1.5.1. 4-(1-Naphthyl)-1-(5-nitrofurfurylidene)semicarbazide (18). Bright-orange needles (52%); mp 236.5–238.0 °C (from acetone) (Found: C, 59.2; H, 3.7; N, 17.0. C₁₆H₁₂N₄O₄ requires C, 59.3; H, 3.7; N, 17.3); δ_H (400 MHz, acetone-d₆) 7.29 (1H, d, J 3.9, furan-*H*), 7.52 (1H, t, J 7.9, naphthyl-*H*), 7.58 (1H, dt, J_1 8.0, J_2 1.0, naphthyl-*H*), 7.64 (1H, dt, J_1 8.3, J_2 1.4, naphthyl-*H*), 7.65 (1H, d, J 3.9, furan-*H*), 7.74 (1H, d, J 8.2, naphthyl-*H*), 7.96 (1H, d, J 8.0, naphthyl-*H*), 8.05 (1H, d, J 7.8, naphthyl-*H*), 8.11 (1H, d, J 8.3, naphthyl-*H*), 8.12 (1H, s, –CH=N), 9.14 (1H, s, NH) and 10.43 (1H, s, NH); δ_C (100 MHz, acetone-d₆) (HMQC, HMBC) 113.09 (furan-C), 114.12 (furan-C), 119.12, 119.33, 121.43, 124.78, 126.34, 126.52, 127.58, 128.87, 133.80, 134.67 (naphthyl-C), 128.91 (H-C=N), 151.00 (furan-C), 152.82 (furan-C) and 152.93 (–C=O); m/z 324 (M⁺, 59.2%), 169 (85.8), 155 (100.0) and 143 (70.5).

6.1.5.2. 4-(2-Naphthyl)-1-(5-nitrofurfurylidene)semicarbazide (19). Bright-orange needles (56%); mp 129.0–130.5 °C (from acetone:MeOH) (Found: C, 59.25; H, 3.7; N, 17.2. C₁₆H₁₂N₄O₄ requires C, 59.3; H, 3.7; N, 17.3); δ_H (400 MHz, DMSO-d₆) 7.40 (1H, dt, J_1 7.9, J_2 1.0, naphthyl-*H*), 7.43 (1H, d, J 4.0, furan-*H*), 7.48 (1H, dt, J_1 8.1, J_2 1.2, naphthyl-*H*), 7.75 (1H, dd, J_1 8.8, J_2 2.0, naphthyl-*H*), 7.81–7.85 (3H, m, furan-*H* + naphthyl-*H* + naphthyl-*H*), 7.87 (1H, d, J 9.0, naphthyl-*H*), 7.96 (1H, s, –CH=N), 8.20 (1H, d, J 1.7, naphthyl-*H*), 9.14 (1H, s, NH) and 11.30 (1H, s, NH); δ_C (100 MHz, DMSO-d₆) (HMQC, HMBC) 113.74 (furan-C), 116.02 (furan-C), 116.45, 121.77, 125.29, 127.20, 127.98, 128.31, 128.98, 130.49, 134.29, 137.20 (naphthyl-C), 129.88 (H-C=N), 152.00 (furan-C), 153.34 (furan-C) and 153.61 (–C=O); m/z 324 (M⁺, 35.0%), 169 (86.0), 155 (38.1) and 143 (100.0).

6.2. Biology

6.2.1. Anti-trypanosomal bioassays

T. cruzi epimastigotes (Tulahuen 2 strain) were grown at 28 °C in an axenic medium (BHI-Tryptose) complemented with 10% fetal calf serum. Cells from a 10-day old culture (stationary phase) were inoculated into 50 cm³ of fresh culture medium to give an initial concentration of 1 × 10⁶ cells/cm³. Cell growth was followed every day by measuring the absorbance of the culture at 600 nm. Before inoculation, the medium was supplemented with the indicated amount of the drug from a stock solution in DMSO. The final concentration of DMSO in the culture media never exceeded 0.4% and the control was run in the presence of 0.4% DMSO and in the absence of any drug. No effect on epimastigote growth was observed with the presence of up to 1% DMSO in the culture media. The percentage of inhibition was calculated as follows: % = {1 – [(A_p – A_{0p})/(A_c – A_{0c})]} × 100, where A_p = A₆₀₀ of the culture containing the drug at day 5;

$A_{0p} = A_{600}$ of the culture containing the drug just after addition of the inocula (day 0); $A_c = A_{600}$ of the culture in the absence of any drug (control) at day 5; $A_{0c} = A_{600}$ in the absence of the drug at day 0.

6.2.2. ED_{50} determination

ED_{50} values were determined by following 50% effective doses to inhibit the parasite growth in the absence (control) and presence of increasing concentrations of the corresponding drug. At day 5, the absorbance of the culture was measured and the percentage of inhibition was calculated. The ED_{50} value was taken as the concentration of drug needed to reduce the growth ratio to 50%.

6.3. Molecular modeling

The docking analysis was carried out on the trypanothione-binding site of *T. cruzi* trypanothione reductase (Structure 1BZL, EC: 1.6.4.8, from RCSB Protein Data Bank, <http://www.rcsb.org/pdb>) where the residues were bonded more closely to the natural substrate. The natural substrate was extracted from the complex, and during the calculations only the residues and water molecules in contact with trypanothione (at a distance of 5 Å) were included in the active site. Those residues were G14, S15, G16, L18, E19, W22, N23, C53, V54, V59, K62, I107, S110, Y111, M114, T335, P336, I339, F396', T397', P398', L399', M400', K402', T457', I458', G459', V460', H461', P462', T463', S464', E466', E467', C469', S470', R472'. The N^1 , C^2 and C^3 atoms of the indolyl group of the W22 residue in the binding site were positioned at (27.86, 4.88, 1.80 Å), (27.64, 5.06, 3.15 Å) and (28.41, 4.19, 3.87 Å), respectively.

The analysis of nitrofurazone derivative **1** as a ligand onto the active site of the enzyme was carried out by means of the FLEXIDOCK [46,52] program from the BIOPOLYMER module of SYBYL and using the default parameters. The maximum number of generations allowed was 3000. The active site was treated as a rigid molecule whereas the ligand was treated as being flexible.

The ligand–cavity binding energy (E) was obtained from the DOCK program by minimization of the ligand into the rigid TR cavity using the Tripos force field [53], a gradient termination of $0.05 \text{ kcal mol}^{-1} \text{ \AA}^{-1}$ and following the Powell method. Compounds **2**, **4**, **5**, **10**, **11**, **16**, **17**, **21**, and **22** were initially positioned within the active site of TcTR in a similar disposition to the best orientation of nitrofurazone **1**. These arrangements were then optimized using the DOCK command. Charges for the ligand were obtained from Gasteiger–Marsili and Hückel methods whereas the site charges were obtained using the Kollman force field [54] as implemented within SYBYL. During minimization, a low dielectric model ($\epsilon = 1$) with a distance-dependent dielectric function was used because we assumed hydrogen bonds to be crucial for the binding. The region where the minimization was carried out has lower and higher corners at (4.00, –12.00, –6.00 Å) and (32.00, 12.00, 12.00 Å), respectively. The term E was

obtained by subtracting the energies of the cavity and the absolute minimum of the ligand from the energy of the ligand–cavity complex from the DOCK program (the former value was calculated by the corresponding conformational analysis of the compound excluding conformations with intramolecular hydrogen bonds as these are improbable in aqueous media). The loss of translational and rotational entropy for the ligand was not considered because semi-empirical quantum-mechanical AM1 [55] calculations reflected the fact that entropies of the studied ligands were essentially the same (42.4 ± 0.2 and $34.3 \pm 0.8 \text{ cal mol}^{-1} \text{ K}^{-1}$, respectively) and therefore, they should not contribute significantly to the discrimination between ligands in this series.

The cavity–ligand binding energy including desolvation energy (BE) was estimated by means of the LEAPFROG module of SYBYL [46] in the same region as used in the docking analysis, with default values used for the keywords. In LEAPFROG the binding energy is calculated from three major components: the direct steric, electrostatic, and implicit hydrogen bonding enthalpies of ligand–cavity binding, all of which were calculated using the Tripos force field [53]. The program also allows the use of optional cavity and ligand desolvation energies, estimated from a very simple model. In general, the method used to calculate binding energies in LEAPFROG is similar to that in Goodford's GRID program [56]. However, in LEAPFROG, the ligand atom coordinates are binned to increase speed and the binding energy of each ligand atom is calculated as though the atom were actually located in the center of a cube containing that atom. A simple linear expression correlates the energy of interaction between the site and that particular ligand atom. Summing over all ligand atoms yields the overall site–ligand interaction energy. In a previous test carried out by us, LEAPFROG desolvation energies (E_D) of formaldehyde, methanol, water, nifuroxim, nitrofurazone **20** and its butyl derivative **1** showed a good correlation ($E_D^{\text{SM2-AM1}} = 2.790 + 0.783 E_D^{\text{LEAPFROG}}$; $r^2 = 0.953$, S.E. = 1.46, $p = 0.001$, $q^2 = 0.871$, S.E. = 2.42) with the corresponding desolvation energies from a semi-empirical quantum-mechanical method 1SCF SM2-AM1//AM1 [47] (wavefunction//geometry) included in the AMSOL package [57].

The Gibbs free energies of the single-electron reduction for the ligands were calculated in the gas phase at 298 K using the AM1 [55] method (keywords = force thermo(298,298) rot = 1 doublet). $\Delta G(L^-)$ values in Tables 1 and 4 are the result of subtracting the Gibbs free energy of the neutral ligand from that in corresponding anion radical. Geometries were fully optimized in all calculations.

Molecular coordinates and charges (SYBYL mol2 files) are available upon request (merino@unavarra.es).

Acknowledgements

Financial support from Fondo Clemente Estable and C.S.I.C.-UDELAR (Uruguay) is acknowledged. H.C. thanks

the C.S.I.C.-UDELAR (Uruguay) and A. Duffaut thanks PEDECIBA-QUÍMICA (Uruguay) for fellowships.

References

- [1] S.L. Croft, *Mem. Inst. Oswaldo Cruz* 94 (1999) 215–220.
- [2] J.C. Messeder, L.W. Tinoco, J.D. Figueroa-Villar, E.M. Souza, R. Santa Rita, S.L. de Castro, *Bioorg. Med. Chem. Lett.* 5 (1995) 3079–3080.
- [3] J.A. Urbina, *Curr. Pharm. Des.* 8 (2002) 287–295.
- [4] J.A. Castro, E.G. Díaz de Toranzo, *Biomed. Environ. Sci.* 1 (1988) 19–33.
- [5] N.B. Gorla, O.S. Ledesma, G.P. Barbieri, I.B. Larripa, *Mutat. Res.* 224 (1989) 263–267.
- [6] Available from <http://www.who.int/tdr/>.
- [7] H. Cerecetto, M. González, *Curr. Topics Med. Chem.* 2 (2002) 1185–1211.
- [8] J. Tovar, M.L. Cunningham, A.C. Smith, S.L. Croft, A.H. Fairlamb, *Proc. Natl. Acad. Sci. USA* 95 (1998) 5311–5316.
- [9] L. Salmon-Chemin, E. Buisine, V. Yardley, S. Kohler, M.A. Debreu, V. Landry, C. Sergheraert, S.L. Croft, R.L. Krauth-Siegel, E. Davioud-Charvet, *J. Med. Chem.* 44 (2001) 548–565.
- [10] S. Girault, T.E. Davioud-Charvet, L. Maes, J.F. Dubremetz, M.A. Debreu, V. Landry, C. Sergheraert, *Bioorg. Med. Chem.* 9 (2001) 837–846.
- [11] A. Schmidt, R.L. Krauth-Siegel, *Curr. Topics Med. Chem.* 2 (2002) 1239–1259.
- [12] R.H. Schirmer, J.G. Müller, R.L. Krauth-Siegel, *Angew. Chem., Int. Ed. Engl.* 34 (1995) 141–154.
- [13] C. Chan, H. Yin, J. Garforth, J.H. McKie, R. Jaouhari, P. Speers, K.T. Douglas, P.J. Rock, V. Yardley, S.L. Croft, A.H. Fairlamb, *J. Med. Chem.* 41 (1998) 148–156.
- [14] M.O.F. Khan, S.E. Austin, C. Chan, H. Yin, D. Marks, S.N. Vaghjiani, H. Kendrick, V. Yardley, S.L. Croft, K.T. Douglas, *J. Med. Chem.* 43 (2000) 3148–3156.
- [15] B. Bonnet, D. Soulez, S. Girault, L. Maes, V. Landry, T.E. Davioud-Charvet, C. Sergheraert, *Bioorg. Med. Chem.* 8 (2000) 95–103.
- [16] Z. Li, M.W. Fennie, B. Ganem, M.T. Hancock, M. Kobaslija, D. Rattendi, C.J. Bacchi, M.C. O'Sullivan, *Bioorg. Med. Chem. Lett.* 11 (2001) 251–254.
- [17] G.B. Henderson, P. Ulrich, A.H. Fairlamb, I. Rosenberg, M. Pereira, M. Sela, A. Cerami, *Proc. Natl. Acad. Sci. USA* 85 (1988) 5374–5378.
- [18] K. Blumenstiel, R. Schoneck, V. Yardley, S.L. Croft, R.L. Krauth-Siegel, *Biochem. Pharmacol.* 58 (1999) 1791–1799.
- [19] R. Docampo, S.N.J. Moreno, A.O.M. Stoppani, W. Leon, F.S. Cruz, F. Villalta, R.P.A. Muniz, *Biol. Pharmacol.* 30 (1981) 1947–1951.
- [20] R. Docampo, S.N.J. Moreno, in: W.A. Pryor (Ed.), *Free Radicals in Biology*, Academic Press, New York, 1984, pp. 243–288.
- [21] L.J. Vergara, J.A. Squella, J. Aldunate, M.E. Letelier, S. Bollo, Y. Repetto, A. Morello, P.L. Spencer, *Bioelectrochem. Bioenerg.* 43 (1997) 151–156.
- [22] C. Olea-Azar, A.M. Atria, R. Di Maio, G. Seoane, H. Cerecetto, *Spectrosc. Lett.* 31 (1998) 849–857.
- [23] J.D. Maya, S. Bollo, L.J. Nunez-Vergara, J.A. Squella, Y. Repetto, A. Morello, J. Perie, G. Chauviere, *Biochem. Pharmacol.* 65 (2003) 999–1006.
- [24] H. Cerecetto, R. Di Maio, G. Ibarri, G. Seoane, A. Denicola, G. Peluffo, C. Quijano, M. Paulino, *Farmaco* 53 (1998) 89–94.
- [25] H. Cerecetto, R. Di Maio, M. González, M. Risso, G. Sagrera, G. Seoane, A. Denicola, G. Peluffo, C. Quijano, M.A. Basombrío, A.O.M. Stoppani, M. Paulino, C. Olea-Azar, *Eur. J. Med. Chem.* 35 (2000) 343–350.
- [26] C. Olea-Azar, A.M. Atria, F. Mendizabal, R. Di Maio, G. Seoane, H. Cerecetto, *Spectrosc. Lett.* 31 (1998) 99–109.
- [27] V. Martínez-Merino, H. Cerecetto, *Bioorg. Med. Chem.* 9 (2001) 1025–1030.
- [28] N. Cenas, D. Bironaite, E. Dickancaite, Z. Anusevicius, J. Sarlauskas, J.S. Blanchard, *Biochem. Biophys. Res. Commun.* 204 (1994) 224–229.
- [29] C.S. Bond, Y. Zhang, M. Berriman, M.L. Cunningham, A.H. Fairlamb, W.N. Hunter, *Struct. Fold Des.* 7 (1999) 81–89.
- [30] S. Bailey, K. Smith, A.H. Fairlamb, W.N. Hunter, *Eur. J. Biochem.* 213 (1993) 67–75.
- [31] S. Bonse, C. Santelli-Rouvier, J. Barbe, R.L. Krauth-Siegel, *J. Med. Chem.* 42 (1999) 5448–5454.
- [32] P.A. Karplus, G.E. Schulz, *J. Mol. Biol.* 210 (1989) 163–180.
- [33] L.A. Carpino, B.A. Carpino, A.G. Chester, R.W. Murray, A.A. Santilli, P.H. Terry, *Organic Synthesis Collective*, Vol 5, 1973, pp. 168–170, John Wiley & Sons.
- [34] S. Rajagoplan, P. Raman, *Organic Synthesis Collective*, 1995, Vol 3, pp. 425–427, John Wiley & Sons.
- [35] M.O. Abdel-Rahman, M.N. Aboul-Enein, W.M. Tadros, *J. Chem. UAR* 12 (1969) 69–75.
- [36] M. Bodanzky, A. Bodanzky, *The Practice of Peptide Synthesis*, second ed, Longman Group Limited, London, 1978.
- [37] H. Cerecetto, R. Di Maio, M. González, G. Seoane, *Heterocycles* 45 (1997) 2023–2028.
- [38] H. Cerecetto, R. Di Maio, M. González, M. Risso, P. Saenz, G. Seoane, A. Denicola, G. Peluffo, C. Quijano, C. Olea-Azar, *J. Med. Chem.* 42 (1999) 1941–1950.
- [39] G. Aguirre, H. Cerecetto, R. Di Maio, M. González, G. Seoane, A. Denicola, M.A. Ortega, I. Aldana, A. Monge, *Arch. Pharm.* 335 (2002) 15–21.
- [40] J. Rodríguez Coura, S.L. De Castro, *Mem. Inst. Oswaldo Cruz* 97 (2002) 3–24.
- [41] J.F. Faucher, T. Baltz, K.G. Petry, *Parasitol. Res.* 81 (1995) 441–443.
- [42] M. Almeida-de-Faria, E. Freymuller, W. Colli, M.J. Alves, *Exp. Parasitol.* 92 (1999) 263–274.
- [43] K.M. Tyler, D.M. Engman, *Int. J. Parasitol.* 31 (2001) 472–481.
- [44] ClogP version 4.0 (1999), BioByte Corp., 201 W. Fourth St., Suite#204, Claremont, CA 91711, USA. Available from <http://www.biobyte.com>.
- [45] N. Cenas, A. Nemeikaite-Ceniene, E. Sergediene, H. Nivinskas, Z. Anusevicius, J. Sarlauskas, *Biochem. Biophys. Acta* 1528 (2001) 31–38.
- [46] SYBYL v. 6.8 (2001), Tripos Associates, 1699 South Hanley Road, Suite 303, St. Louis, Missouri 63144.
- [47] C.J. Cramer, D.G. Truhlar, *Science* 256 (1992) 213–217.
- [48] D.B. Jordan, G.S. Basarab, D.I. Liao, W.M. Johnson, K.N. Winzenberg, D.A. Winkler, *J. Mol. Graph. Model.* 19 (2001) 434–447.
- [49] N.V. Belkina, V.S. Skvortsov, A.S. Ivanov, A.I. Archakov, *Vopr. Med. Khim.* 44 (1998) 464–473.
- [50] J.D. Maya, Y. Repetto, M. Agosin, J.M. Ojeda, R. Tellez, C. Gaule, A. Morello, *Mol. Biochem. Parasitol.* 86 (1997) 101–106.
- [51] H. Cerecetto, M. González, M. Risso, G. Seoane, A. López de Ceráin, O. Ezpeleta, A. Monge, L. Suescun, A. Mombrú, A.M. Bruno, *Arch. Pharm.* 333 (2000) 387–393.
- [52] M. Bertelli, E. El-Bastawissy, M.H. Knaggs, M.P. Barrett, S. Hanau, I.H. Gilbert, *J. Comput. Aided Mol. Des.* 15 (2001) 465–475.
- [53] M. Clark, R.D. Cramer III, N. Van Opdenbosch, *J. Comp. Chem.* 10 (1989) 982–1012.
- [54] D. Hall, N. Pavitt, *J. Comp. Chem.* 5 (1984) 441–450.
- [55] J.J.P. Stewart, *J. Comput. Aided Mol. Des.* 4 (1990) 1–105.
- [56] P.J. Goodford, *J. Med. Chem.* 28 (1985) 849–857.
- [57] AMSOL, QCPE Program No. 606 version 4.5, Quantum Chemistry Program Exchange, Indiana University, Bloomington, Indiana USA.